Fine Chemical Engineering
http://ojs.wiserpub.com/index.php/FCE/

Review

Trends on the Development of Hybrid Supercapacitor Electrodes from the Combination of Graphene and Polyaniline

Shella Permatasari Santoso[1,2*], Harry Kasuma (Kiwi) Aliwarga[3], Livy Laysandra[2], Artik Elisa Angkawijaya[4], Felycia Edi Soetaredjo[1,2], Jindrayani Nyoo Putro[1], Maria Yuliana[1], Felix Pasila[5], Kuan-Chen Cheng[6,7,8,9], Hsien-Yi Hsu[10,11,12], Suryadi Ismadji[1,2]

[1]Department of Chemical Engineering, Faculty of Engineering, Widya Mandala Surabaya Catholic University, Surabaya, East Java, Indonesia
[2]Department of Chemical Engineering, National Taiwan University of Science and Technology, Taipei, Taiwan
[3]UMG IdeaLab, Myanmar
[4]Graduate Institute of Applied Science and Technology, National Taiwan University of Science and Technology, Taipei, Taiwan
[5]Electrical Engineering Department, Petra Christian University, Surabaya, East Java, Indonesia
[6]Institute of Food Science and Technology, National Taiwan University, Taipei, Taiwan
[7]Institute of Biotechnology, National Taiwan University, Taipei, Taiwan
[8]Department of Medical Research, China Medical University Hospital, China Medical University, Taichung, Taiwan
[9]Department of Optometry, Asia University, Taichung, Taiwan
[10]School of Energy and Environment, City University of Hong Kong, Tat Chee Avenue, Kowloon Tong, Hong Kong, China
[11]Department of Materials Science and Engineering, City University of Hong Kong, Tat Chee Avenue, Kowloon, Hong Kong, China
[12]Shenzhen Research Institute of City University of Hong Kong, Shenzhen, China
E-mail: shella_p5@yahoo.com, shella@ukwms.ac.id

Received: 2 August 2021; **Revised:** 8 December 2021; **Accepted:** 27 December 2021

Abstract: The high demand for efficient energy devices leads to the rapid development of energy storage systems with excellent electrochemical properties, such as long life cycles, high cycling stability, and high power density. SC is postulated as a potential candidate to fulfill this demand. The combination of graphene and polyaniline can create SC electrodes with excellent electrical conductivity, high specific surface area, and high capacitance. The graphene/polyaniline hybrid electrodes represent an attractive means to overcome the major drawbacks of graphene or polyaniline non-hybrid (single) electrode materials. In this review article, the trend in the development of various graphene/polyaniline hybrid electrodes is summarized, which includes the zero-dimension graphene-quantum-dots/polyaniline hybrid, one-dimension graphene/polyaniline hybrid, two-dimension graphene/polyaniline hybrid, and three-dimension hydrogel-shaped graphene/polyaniline hybrid. Several strategies and approaches to enhance the capacitance value and cycling stability of graphene/polyaniline hybrid electrodes are discussed in this review article, such as the addition of transition metal oxides and metal-organic frameworks, and modification of graphene into functionalized-graphene. The performance of the electrodes prepared from the combination of graphene with other conducting polymers (i.e., polypyrrole, polythiophene, and polythiophene-derivatives) is also discussed.

***Keywords*:** hybrid electrode, nanocomposite, graphene polyaniline, conducting polymer, asymmetric supercapacitor

DOI: https://doi.org/10.37256/fce.3120221077

Graphical abstract

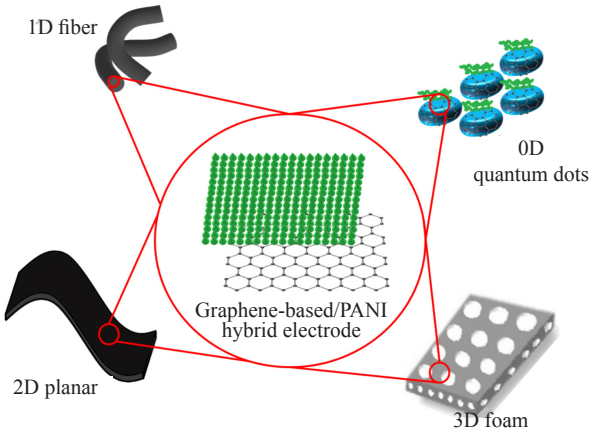

Nomenclature

Abbreviation	Definition
0D	zero-dimension
1D	one-dimension
2D	two-dimension
3D	three-dimension
AAm	acrylamide
AEESC	active electrolyte-enhanced supercapacitor
ANI	aniline
APS	ammonium persulfate
ATRGO	amino triazine functionalized-reduced graphene oxide
BTC	1,3,5-benzene tricarboxylic
BET	Brunauer-Emmett-Teller
BDC	1,4-benzene dicarboxylic
CC	carbon cloth
CFC	carbon fiber cloth
CNT	carbon nano tube
CP	conducting polymer
CSA	camphorsulfonic acid
CT	cotton
CV	cyclic voltammogram
CVD	chemical vapor deposition
EDLS	electrical double-layer supercapacitor
EMITFSI/PVDF-HFP	ionic liquid/poly (vinylidenefluoride-co-hexafluoropropylene)
ESD	energy storage device
F-GnO	fluoro-functionalized graphene oxide
FS	Faradaic supercapacitor
Gn or G	graphene
GCE	glassy carbon electrode
G-PC	graphene-grafted PANI copolymer
GFP	graphene/Fe_2O_3/PANI
GH	graphene hydrogel

GO	graphene oxide
GNS	graphene nanosheet
GP	graphene paper
G/PANI	graphene/PANI
GNS	graphene nanosheet
GOF	fluoro-functionalized graphene oxide
GQD	graphene quantum dot
Gt	graphite
HS	hollow sphere
LbL	layer-by-layer
LiB	lithium battery
MOF	metal-organic framework
MWCNT	multi-walled carbon nano tube
NH_2-Gn	aminated graphene
NH_2-GNS	amine-functionalized graphene nanosheets
NSA	1,5-naphthalene sulfonic acid
NW	nanowhiskers
OMC	ordered-mesoporous-carbon
PAAm	polyacrylamide
PAG	*p*-aminophenol functionalized-graphene
PAN	polyacrylonitrile
PANI	polyaniline
PCBM	phenyl-C60-butyric acid methyl ester
PDMS	polydimethylsiloxane
PEDOT	poly (3,4-ethylenedioxythiophene)
PET	polyester fabric
PMMA	poly (methyl methacrylate)
PPDA	*p*-phenylenediamine
PPy	polypyrrole
PS	polystyrene
PTA	*p*-benzene dicarboxylic acid
PTh	polythiophene
PVA	polyvinyl alcohol
PVDF	polyvinylidene difluoride
RFC	resorcinol-formaldehyde carbon
RGO	reduced graphene oxide
RGOH	reduced graphene oxide hydrogel
SC	supercapacitor
SEM	scanning electron microscopy
S-Gn	sulfonated graphene
S,N:GQD	sulfur, nitrogen-functionalized graphene quantum dot
SS	solid state
SSA	specific surface area
TCTA	2,4,6-trichloro-[1,3,5] triazine
TEM	transmission electron microscopy
Th	thiophene
THF	tetrahydrofuran
TMO	transition metal oxide
TPA	triphenylamine
XPS	X-ray photoelectron spectroscopy

XRD X-ray diffraction

1. Introduction

SCs, also referred to as ultracapacitors, are a type of ESD with high power density, fast charge-discharge rate, and long life-cycle.[1-3] SCs are constructed from a sandwich of two electrodes and are separated by a porous membrane imbibed by the electrolyte in a solid, liquid, or quasi-solid state.[4-7] SCs are considered safer than batteries, owing to their lower heating rate, better mechanical properties, and higher stability.[8] The lightweight and flexible structure of SC also adds to its appeal as an ESD.[9] SCs are widely used as regenerative-braking systems in hybrid cars and electric vehicles, energy storage, and power delivery for wearable or portable electronic devices.[10-11] Despite their remarkable abilities, the relatively low energy density of SCs remains a persistent challenge in the field and their development.

SCs can be classified into two categories based on the energy storage mechanisms, FS and EDLS.[2,12] The charging mechanism of an EDLS is based on the reversible electrostatic attraction between the charged surface of electrodes and the electrolyte ions. In this regard, electrode materials with high SSA and controlled-pore sizes are required to establish EDLSs with high energy storage capacity and specific capacitance values, wherein hierarchical-porous activated carbons are generally employed.[13-14] Alternatively, FS stores charges based on the fast and reversible Faradaic (redox) reactions on the electrode surface.[15] Combining transition metals and CPs is one of the most commonly used approaches to construct working electrode materials for FSs.[16] However, FSs often suffer from poor electrical conductivity than EDLSs since Faradaic reactions are generally slower than the non-Faradaic process, which eventually leads to poor cycling stability.[12,15] The combination of carbon-based materials and CPs in preparing the hybrid SC electrodes creates an asymmetric behavior, leading to high cycling stability and energy storage capacity.[17]

The electrochemical performance of SCs is strongly dependent on the electrode materials.[18] An ideal SC electrode should possess the following criteria: high SSA, controlled porosity, high electrical conductivity, high thermal and chemical stability, environmental friendliness, and low cost.[18-19] Gn, a carbon-based material with a honeycomb monolayer structure, represents a promising candidate as the electrode material for SCs.[20-21] Gn consists of all-sp^2-hybridized carbon, contributing to its electron delocalization and high thermal and electrical conductivity. Gn is also known for its other superior properties, which includes its lightweight, high mechanical strength (~1 TPa), good physical and chemical stability, and high surface area (~2,630 m^2/g).[21-23] The fresh-single layer of Gn is known to have a high theoretical specific capacitance of ~21 uF/cm^{-2}.[12] However, it is still a major challenge to achieve such the maximum capacitance of Gn since its layers tend to encounter severe agglomeration during their preparation and utilization; thus, the expected capacitance value is far from being achieved.[12,24]

The addition of CPs can prevent the agglomeration of Gn (and vice versa), especially during the preparation step. CPs themselves have been widely utilized in the preparation of ESDs. Among the CPs, PANI has received considerable attention due to its good electrical properties and thermal stability that contribute to high capacitance. PANI can produce electrode materials with high specific capacitance values, often higher than EDLSs; however, the resulting SCs exhibit poor cycling stability and low mechanical stability. Therefore, the hybridization of Gn and PANI, to result in G/PANI, has been actively pursued to construct electrode materials to overcome the major drawback of using PANI or Gn alone. In this context, the G/PANI hybrid electrodes can achieve 2-5 times higher specific capacitance values than those of corresponding individual components. Furthermore, the G/PANI hybrid electrodes possess increased electrochemical active sites, facilitating the electrochemical reactions in SCs.[25] The performance of several G/PANI-based electrodes is given in Table 1.

Although G/PANI hybrid electrodes have been extensively developed with potential commercial applications, research is still widely conducted to enhance electrochemical properties. This review summarizes the trend in the development of G/PANI hybrid electrodes and reviews the strategies to improve the electrocapacitive properties of G/PANI hybrid electrodes. This review begins by discussing the performance of various G/PANI electrodes, followed by the developed fabrication methods of enhancing the electrode capacitance. Next, several strategies to improve the G/PANI capacitance are discussed, including adding functional groups to Gn and incorporating TMOs and MOFs. The hybrid electrodes based on the combination of Gn and other CPs are summarized to compare their electrocapacitive performances with G/PANI.

Table 1. Electrocapacitive energy storage properties of Gn/CP-based hybrid electrodes

Material	Electrolyte	Discharge Rate	Specific Capacitance (F/g)	Retention % (Cycle)	U (Wh/kg)	S (W/kg)	Ref.
			G/PANI hybrid				
GQD/PANI	0.5 M H_2SO_4	1 A/g	~1,044	~80.1 (3,000)	117.45	448.8	26
G/PANI	EMITFSI/PVDF-HFP*	0.22 mA/cm^2	87.8 mF/cm^2	10,000	12.2 μW h/cm^2	226.4 μW/cm^2	27
G/PANI	0.5 M H_2SO_4	0.2 mA/cm^2	176 mF/cm^2	74.8 (500)	17.1 μW h/cm^2	0.25 mW/cm^2	28
G/PANI	2 M H_2SO_4	0.1 A/g	500				29
G/PANI	1 M KOH	0.1 A/g	578.8				30
G/PANI	1 M H_2SO_4	1 A/g	763	82 (1,000)			31
G/PANI	1 M H_2SO_4	1 A/g	789.9	90 (5,000)	32.2	793.3	32
G/PANI@Fabric	1 M H_2SO_4	1 A/cm^2	790 F/cm^2	88.9 (5,000)	28.21 μW h/cm^2	0.12 mW/cm^2	33
G/PANI@Cloth	1 M H_2SO_4	5 mV/s	246 mF/cm^2	98 (3,800)	9.7 μW h/cm^2	840.9 μW/cm^2	34
G/PANI@CC	1 M H_2SO_4	0.5 A/g	793	81 (10,000)	11.38	199.8	35
Holey-G/PANI/G	1 M H_2SO_4	1 A/g	437	84 (5,000)	55	900	36
GO/PANI	1 M H_2SO_4	1 mA	429	1,000			37
GO/PANI/paper fiber	0.5 M H_2SO_4	1 A/g	937	74.5 (2,000)	10.12	456	38
RGO/PANI	1 M H_2SO_4	2 mV/s	159.62	82.02 (1,000)	0.31	1,178.78	39
RGO/PANI	1 M H_2SO_4	1 A/g	432	85 (10,000)	25	681	40
RGO/PANI	1 M H_2SO_4	0.5 A/g	438.8	76.5 (2,000)			41
RGO/PANI	PVA/H_2SO_4*	0.5 A/g	424.4	>80 (2,500)			42
RGO-HT/PANI	1 M H_2SO_4	0.2 A/g	420	80 (6,000)	9.3	11,600	10
RGOHG/PANI	AEESC	2.6 A/g	1,120	91.4 (4,000)			43
RGO-Foam/PANI	1 M H_2SO_4	1 A/g	790	80 (5,000)	17.6	98	44
RGO/PANI/RFC	6 M KOH	1 A/g	523	87.6 (5,000)			45
			Functionalized-G/PANI hybrid				
S,N:GQD/PANI@Ni-Foam	2 M KOH	2-10 A/g	2,524-1,699	100 (1,000)	71	450	46
GO/PANI/eCFC	1 M H_2SO_4	1 A/g	940				47
RGO/PANI/eCFC	1 M H_2SO_4	1 A/g	1,145	84 (5,000)	25	92,200	47
N-doped RGO/PANI	1 M H_2SO_4	0.1 A/g	590	100 (200)			48
			G/PANI hybrid with the addition of TMOs				
G/$CoFe_2O_4$/PANI	1 M KOH	0.1 A/g	716.4	96 (5,000)	79.7	178.2	30
G/Fe_2O_3/PANI	1 M KOH		638	92 (5,000)	17	351	49
GO/Mn_3O_4/PANI	1 M H_2SO_4	0.3 A/g	829	94 (1,800)	121	891	25
RGO/Fe_2O_3/PANI@CC	1 M H_2SO_4	0.25 A/g	1,124	82 (10,000)	14.4	58	50
RGO/MnO_2/PANI/Cotton	1 M H_2SO_4	15 A/g	888	70 (3,000)			51
RGO/RuO_2/PANI	1 M H_2SO_4	2 mV/s	723.09	85.14 (1,000)	1.29	215.35	39
RGO/$NiPbTiO_3$/PANI		0.5 A/g	1,180	~91 (10,000)	40		52
RGO/$LaMnO_3$/PANI	PVA-KOH*	2.5 A/g	111	117 (100,000)	35	18,000	53
			Gn hybrid with other CPs				
GO/PPy	1 M KCl	1 A/g	271	64 (>2,000)			54
GO/PPy@MWCNT	1 M Na_2SO_4	100 mV/s	358.69	88.69 (2,000)	40.45	441	55
RGO/PPy	PVA-H_2SO_4*	1 A/g	454	65 (10,000)	48.3	750	56
RGO/PPy@CNT	PVA-H_2SO_4*	10 A/g	443	94.3 (10,000)	7	8.2 mW/cm^2	57
PPy/RGO/PPy@Cu:Ni PET	1 M Na_2SO_4	2 mA/cm^2	684 mF/cm^2	4,000	95 μW h/cm^2	1 mW/cm^2	58
RGO-hydrogel/PPy	1 M KNO_3	3 A/g	340	87.4 (10,000)	46.9	2,400	59
Carboxyl-G/PPy@CNT	1 M KCl	0.5 mA/cm^2	196 mF/cm^2	98.1 (5,000)	10.9 μW h/cm^2	8.1 mW/cm^2	60
G/PPy/MnO_x@$Cu(OH)_2$	6 M KOH	10 mV/s	370	1,000	12/85	6610	61
Co_9S_8/PEDOT:PSS/RGO	2 M KOH	1 A/g	788.9	100 (10,000)	19.6	400.9	62
S-doped GO/PTh	2 M KOH	0.3 A/g	296	91.86 (4,000)	148	41.6	63
RGO/PTh/AgNPs	1 M H_2SO_4	4 mV/s	953.13	91.99 (1,000)	28.8	2,840	64
RGO/PEDOT/PANI	1 M H_2SO_4	1 A/g	535	99 (10,000)	26.89	800	65
PAN/PANI/GQD	0.1 M H_2SO_4	0.67 A/g	589.3				66

*Solid-state electrolyte

2. G/PANI-based hybrid electrodes

2.1 *0D GQD/PANI electrodes*

GQDs are a 0D form of Gn with a particle size of fewer than 10 nm, which possesses several O-containing functional groups such as -COOH and -OH.[67] GQDs are produced through physical or chemical exfoliation of carbon materials (e.g., fullerenes, Gt, Gn, etc.); wherein, a method such as oxidation, hydrothermal treatment, CVD, laser ablation, or plasma treatment is often employed.[68-69] The usage of GQDs alone as the electrode materials has been reported to produce SC with a specific capacitance ranging from 6 F/g to 296.7 F/g.[67,70] Hybridization of PANI with GQDs can result in an SC electrode with enhanced specific capacitance. The presence of GQDs, in an adequate concentration, allows the homogeneous polymerization of ANI into PANI and uniform distribution of the particle size.[68-71]

As an example of GQD/PANI hybridization, Arthisree and Madhuri reported that the hybridization of PANI/GQD with PAN results in PAN/PANI@GQD, and this hybrid electrode can achieve a specific capacitance value of 587 F/g at a current density of 670 mA/g in 0.1 M H_2SO_4 electrolyte.[66] The highest specific capacitance of the GQD/PANI hybrid was reported by Mondal et al.;[26] wherein, the electrochemical characterizations showed a high specific capacitance of 1044 F/g at 1 A/g and 0.5 M H_2SO_4. This group also showed that the addition of GQDs could control the agglomeration of the PANI particles. As revealed by the TEM characterization, agglomeration of PANI particles was observed in the electrode materials prepared without GQDs; the formation of homogeneous PANI nanofibers can be achieved with the addition of GQDs (5-15 wt%). The retardment of PANI polymerization was encountered at a higher number of GQDs addition (i.e., 20 wt%). The highest specific capacitance (1,044 F/g) can be achieved at 10 wt% of GQDs addition, while lower capacitance values (205.7-776.3 F/g) were achieved at other loading amounts of GQDs.

The combination of fullerene and PANI has also been reported to produce SC electrodes with high specific capacitances.[72-74] For instance, outstanding SCs with a specific capacitance of 2201 F/g (at a current density of 2 A/g) have been reported by Ramadan et al. by integrating fullerene with PANI.[73] The hybrid electrode also exhibits superior cycling stability up to 1,000 cycles while maintaining the capacity retention at 96%. In their study, the fullerene/PANI electrode was prepared by mixing 5 mg of PCBM (a fullerene derivative) and 200 µL ANI in 0.5 M H_2SO_4 solution, followed by the addition of ammonium persulfate to polymerize ANI into PANI. They further observed that higher loading amounts of PCBM in the hybrid electrodes led to the formation of large-size PCBM and consequently a decrease in specific capacitance. It also reported that the specific capacitance was lower at high PCBM addition of 10 mg (1,313 F/g, at 2 A/g) and at low PCBM addition of 2.5 mg (1,582 F/g, at 2 A/g). A considerable decrease of specific capacitance at high PCBM addition is due to the formation of large-size PCBM, leading to the reduction of surface area.

Utilizing biomass as a renewable carbon source represents an attractive means to reduce raw material costs in preparing a product. For instance, the utilization of carrot juice as the carbon source in preparing carbon dots has been reported by Oskueyan et al.[75] The carbon dots from carrot juice were mixed with PANI, PPy, and Gn to prepare the composite electrodes. Although biomass-derived material can reduce the raw material cost, the resulting SC electrodes exhibited relatively low stability; wherein, the retention stability is reduced to 62% after only 1,000 cycles. The highest specific capacitance that the electrode composite can reach is 296 F/g (at a current density of 5 A/g). Furthermore, the drawback of using biomass-derived materials is that they may contain some organic impurities, lowering the retention stability.[76]

GQDs show the synergistic effects on the electrochemical performance of CP-based (e.g., PANI) electrodes by controlling the agglomeration of the CPs. Furthermore, the superior electrochemical properties of GQDs emerge due to their high SSA, good electrical conductivity, and plenty of O-containing active groups.

2.2 *1D and 2D G/PANI electrodes*

Flexible, small, thin, and durable are the desired specifications for modern electronic devices, pushing many researches toward developing thin, flexible, and lightweight SCs to substitute conventional bulky and heavy SCs. Flexible SCs typically consist of highly flexible thin-electrodes (e.g., 1D fiber or 2D planar shapes) and are usually supported by soft substrates. In this regard, the flexibility and mechanical robustness of the flexible SCs can be achieved

through strong integration between the flexible substrate and the active electrode material.[77-78]

The 1D fiber or yarn-shaped SC electrodes have a promising application for portable and wearable devices due to their flexibility and tiny volume.[12] A flexible SC based on the G/PANI hybrid fibers obtained from wet spinning has been reported to deliver a high specific capacitance of 87.8 mF/cm^2 at a current density of 0.22 mA/cm^2. This G/PANI hybrid fiber was assembled on a PDMS substrate and then coated with a solid-state electrolyte prepared from the drying of polymer gel to construct a flexible electrode. Zhang et al.[27] showed that Gn to PANI mass ratio plays a crucial factor in determining the capacitance of SC electrodes. For example, G/PANI composite fibers prepared with 0.1 M ANI show a uniform distribution of PANI nanomaterials on the surface of graphene fibers, and the resulting SC has a large capacitance of 55.8 mF/cm^2 at a current density of 0.22 mA/cm^2. On the contrary, the G/PANI composite fibers prepared using 0.3 M ANI resulted in the aggregation of PANI on Gn and thus caused a reduction in the capacitance to 19.3 mF/cm^2. Changing the solid-state electrolyte from PVA/H_3PO_4 into ionic liquid EMITFSI/PVDF-HFP can also be adapted as a strategy to increase the areal capacitance of G/PANI fiber-based electrode. The specific capacitance was increased to 87.8 mF/cm^2 in the presence of an ionic liquid electrolyte.

CC has been widely utilized to prepare flexible two-dimensional SC electrodes, owing to its fibrous characteristic. The preparation method of the composite SC electrodes comprising PANI, Gn, and CC commonly refers to a chemical/electrochemical co-deposition method, as illustrated in Figure 1, and consists of several steps: (1) dipping of CC into aqueous GO dispersion, (2) reduction of GO to RGO (optional), and (3) polymerization of ANI into PANI.[33,35] For example, Wen et al. utilized a cyclic voltammetry to deposit Gn and PANI nanowires on CC to fabricate G/PANI@CC electrode composite exhibiting a specific capacitance of 793 F/g at 0.5 A/g.[35] Lin et al. also reported the preparation of solid-stated SC electrodes through electrodeposition of G/PANI on carbon woven fabric, where a high capacitance of 790 F/cm^2 at 1 A/cm^2 can be achieved by SC.[33]

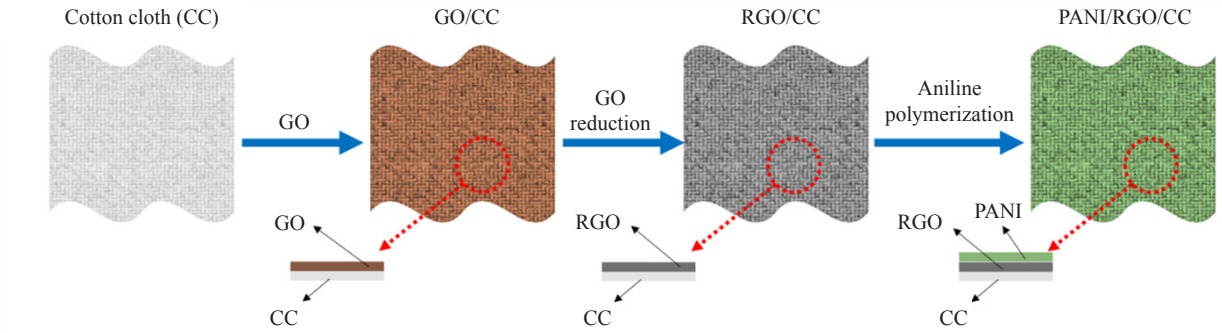

Figure 1. Preparation of flexible SC electrode composites composed of PANI/RGO growth on CC

As another example of a flexible 2D SC electrode, Jin et al.[34] reported a high-performance electrode material from the combination of cotton, Gn, and PANI. In this regard, the G/PANI@cotton electrode was prepared by coating cotton yarns with Gn sheets and PANI nanowire arrays. A combination of PVA/H_3PO_4 was introduced as the doping agent. The resulting solid-state G/PANI@cotton electrode displayed excellent cycling stability up to 3,800 cycles with a loss of capacitance retention of 2%. This flexible electrode has an areal-specific capacitance of 246 mF/cm^2 and an energy density of 9.7 μW h/cm^2 at a power density of 840 μW/cm^2. The flexible 2D electrode can also be prepared by utilizing commercial paper as the substrate reported by Li et al.[28] The G/PANI@paper shows an areal capacitance of 176 mF/cm^2 at a current density of 0.2 mA/cm^2, which is ~10 times larger than that of Gn-paper. Jin et al.[34] also reported a hybrid electrode using the same material combination of Gn, PANI, and paper. This group shows that the amount of PANI deposited on paper can be controlled by controlling the polymerization time; wherein, the electrochemical polymerization time of 900s resulted in a high PANI mass density. The prepared hybrid electrode can achieve a capacitance of 123 mF/cm^2 at a current density of 0.5 A/cm^2. However, the resulting electrode material exhibited a relatively low cycling stability of 500 cycles with capacitive retention of 74.8%. Another work worth mentioning is from Xiao et al.[79]; this group reported the synthesis of RGO/PANI@paper through the deposition of GO and PANI

nanofibers on the A4 paper through the printing technique. The RGO was formed through chemical reduction of GO@paper using HI solution at an electrical conductivity of 340 S/m. The PANI nanofibers were then deposited on the flexible RGO paper by employing electropolymerization of ANI. The resulting flexible thin RGO/PANI@paper can achieve a specific capacitance of 522 F/g at 1 A/g. The addition of another RGO layer on top of RGO/PANI@paper to produce a sandwich-like RGO/PANI/RGO@paper can further improve the specific capacitance to 581 F/g. Meanwhile, RGO@paper achieved a much lower specific capacitance of 55 F/g at the same current density. The resulting RGO/PANI/RGO@paper also demonstrated an enhanced long-term cycling stability (85% capacitive retention) compared to PANI/RGO paper (57% retention) after 10,000 charge-discharge cycles.

The establishment of flexible electronic devices is closely related to the development of stretchable and wearable electrodes. An excellent flexible electrode should be able to withstand mechanical deformation without undergoing electrical failure after bending or twisting. The critical factor in developing an excellent flexible electrode with high SSA is the precise interlayer thickness and uniform distribution of PANI and/or Gn on the substrate, which can be achieved by controlling the polymerization process.

2.3 *3D G/PANI electrodes*

Hydrogel or aerogel represents a 3D, lightweight, and hierarchically porous material with interconnected structure, beneficial for ion transport in SCs.[80-82] Furthermore, hydrogel also has high SSA, which allows the loading of a high number of active materials.[81] Hydrogels from CPs possess high conductivity and excellent stretch-ability, which enables them to withstand structural collapse and extreme volume change during cycling.[82-83] However, CPs-based hydrogels are not sufficiently tolerant of large and complex mechanical deformation. Hybridization of CPs with highly stretchable, compressible, and bendable polymer was postulated as a strategy to overcome this drawback. As an example of this strategy, high mechanical strength and super-elastic hydrogel electrode were successfully produced through cryopolymerization of anisotropic PVA/PANI. This hydrogel has a specific capacitance of 260 F/g and an energy density of 27.5 Wh/kg, and is able to fully recover after undergoing 100% stretching-compressing strain.[83]

Cellulose can serve as natural and low-cost 3D aerogel electrodes;[81,84] the combination of cellulose/GO/PANI can result in an aerogel electrode with an areal specific capacitance of 1,218 mF/cm^2 (at a current density of 1 mA/cm^2).[81] The cellulose/GO/PANI aerogel preparation was initiated by the dissolution of cotton linter pulp in LiBr, followed by the dispersion of GO nanosheets. The PANI nanoclusters were then coated onto the cellulose/GO aerogel through in situ polymerization of ANI.[81] Zhou et al.[85] reported another stretchable Gn-containing hydrogel electrode, wherein PAAm was used as the copolymer of PANI. The resulting PAAm/G/PANI hydrogel shows an areal capacitance of 500.13 mF/cm^2 (at 0.5 mA/cm^2) and 100% capacitance retention after 10,000 cycles. Meanwhile, the PAAm/PANI hydrogel shows four times lower areal capacitance of 114.5 mF/cm^2.

Another method for preparing hydrogel electrode is by fabricating the Gn particles into the 3D hydrogel instead of using a polymer. As an example of this approach, Liu et al.[80] reported the preparation of RGO/PANI hydrogel film. The RGO hydrogel film was prepared by first treating GO with NaOH aqueous solution. The GO-containing solution was then dropped onto a platform stacked with 7 glass sheets in an autoclave reactor surrounded by a few milliliters of water. The reaction then proceeded hydrothermally to obtain the RGO hydrogel film. Subsequently, PANI was deposited on the RGO hydrogel film through electropolymerization of ANI. The RGO/PANI hydrogel film can achieve a specific capacitance of 853.7 F/g (at 1 A/g), and the electrode is able to maintain 92.6% of the capacitance after undergoing 8,000 cycles. Chi et al.[86] have reported the preparation of 3D hierarchical porous RGO/PANI foam. The foam electrode was prepared by the dipping and dry method, as illustrated in Figure 2a. In this context, a low-density three-dimensional metal foam (e.g., Ni- or Cu-foam) was utilized as the template. The alignment of PANI nanowire arrays on the RGO-foam substrate was achieved by the *in situ* polymerization reaction. The resulting composite can drastically increase the electrocapacitive properties, fulfilling a specific capacitance of 864 F/g at 1 A/g with capacitive retention of 85.6% after 5,000 charge/discharge cycles.

The preparation of 3D electrodes in the absence of support materials (known as free-standing electrodes) is another unique approach to preparing lightweight electrodes. Dissolvable polymers, such as PS and PMMA, were commonly used as sacrificial templates. The PS sphere was first employed as a rigid template for molding PANI-HS in such a process. PS was then removed by introducing a dissolving solvent (i.e., THF) to form PANI-HS particles. The schematic illustration showing the stepwise synthesis of PANI-HS is depicted in Figure 2b. For the GO hybridization step, the

negatively charged GO nanosheets were wrapped on the surface of PANI-HS particles and then electrochemically reduced to form PANI-HS@ERGO. The specific capacitance of the resultant composite electrode was 614 F/g at 1 A/g with a 90% capacitance retention after 500 galvanostatic charge-discharge cycles.[87] PMMA is another type of dissolvable polymer that can be utilized as a sacrificial template to prepare PANI-HS.[88]

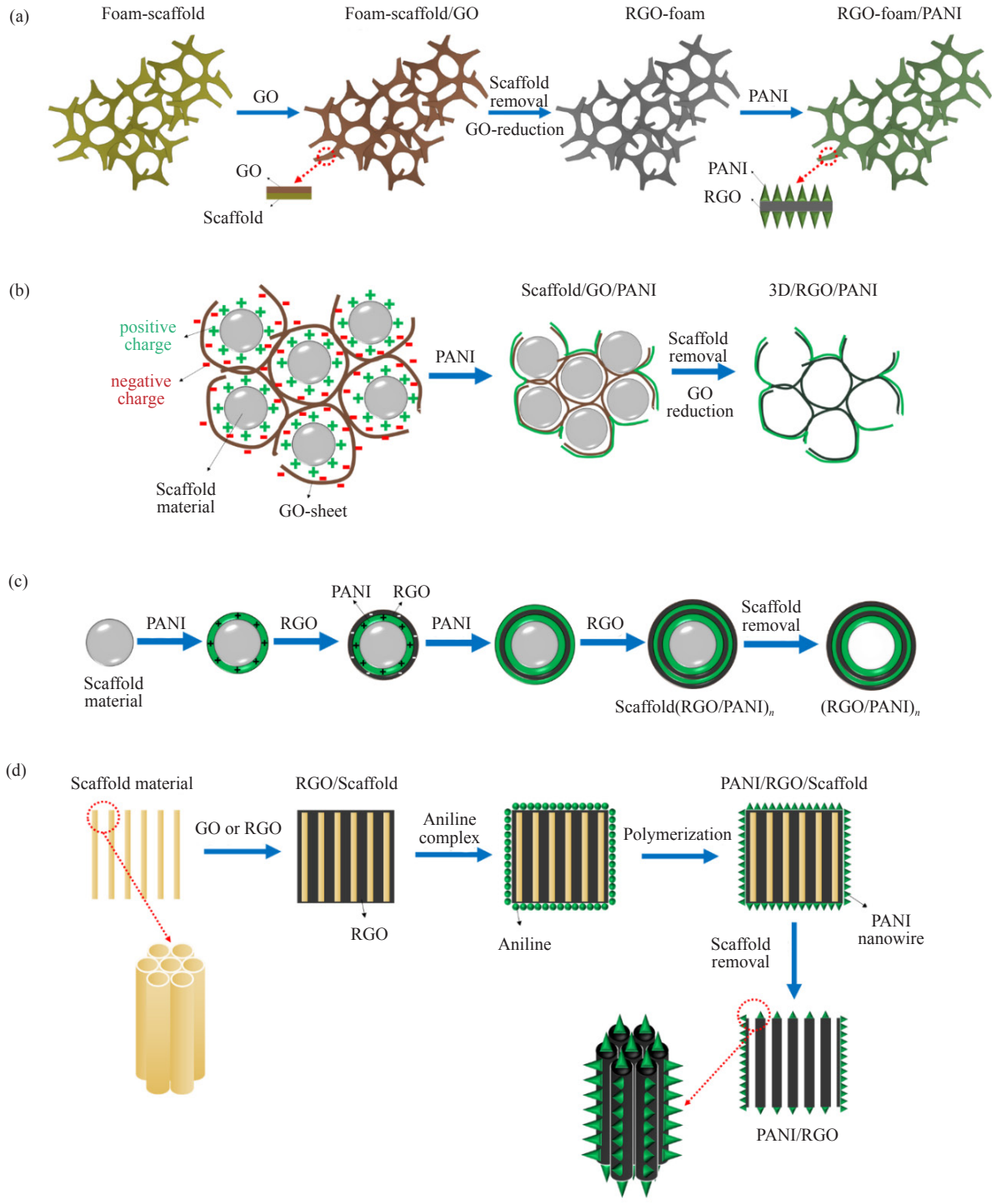

Figure 2. Various techniques to prepare 3D composite electrodes (a) hydrogels or 3D foams as a template to form free-standing electrodes; (b) sacrificial polymer templates to produce hollow composite electrode particles; (c) LbL deposition of PANI and RGO on the sacrificial template; (d) ordered-mesoporous silica to create an ordered-mesoporous carbon

In another study, Luo et al.[89] reported the fabrication of a novel three-dimensional G/PANI hybrid HS by using an LbL assembly technique. The schematic diagram of the LbL preparation method is illustrated in Figure 2c. The prepared composite was utilized as the electrode for SC, yielding a specific capacitance of 381 F/g at a current density of 4 A/g. The resulting SC electrode also exhibits a promising long-term cycling stability with a capacity retention of 83% after 1,000 cycles. Furthermore, the authors claimed that the specific capacitance of the composite could be tailored by changing the assembly cycle number. Combining 3D graphene with a porous structure and conducting PANI possibly still attracts many researchers in the next several years. A hybrid electrode decorated with well-ordered PANI nanowhiskers has been reported by Yan et al.[90] In their study, the ordered-mesoporous silica (SBA-15) impregnated with sucrose/H_2SO_4 solution was used as a template to produce OMC via carbonization at 900 °C. The vertically aligned PANI nanowhiskers were then deposited on the OMC through an oxidative chemical polymerization of ANI. The preparation route of the PANI nanowhiskers/OMC composite is illustrated in Figure 2d. PANI nanowhiskers were first doped with CSA, resulting in an SC device with a specific capacitance of 470 F/g.

3. Strategies to enhance electrochemical properties of G/PANI hybrid electrodes

3.1 *Incorporation of TMOs*

The incorporation of TMO particles has been actively pursued as an effective means to improve the specific capacitance of the G/PANI hybrid electrodes. TMOs consist of transition metals from the *d*-block element with partially-filled *d*-subshell, rendering them good electrical conductivity properties.[91-95] Several TMOs that have been used to enhance the specific capacitances of SCs are Fe_2O_3, Mn_3O_4, RuO_2, MnO_2, and so forth. The usage of nanosized TMOs can improve the electrochemical performance of SCs compared to their bulk counterpart, which can be ascribed to the higher surface area of nanosized TMOs.[96-97]

A ternary nanostructured PANI/RGO/Fe_2O_3 on CC (hereinafter referred to as PANI/RGO/Fe_2O_3@CC) composite hydrogels is reported to produce flexible SC electrode with a specific capacitance of 1124 F/g (at 0.25 A/g).[50] The composite hydrogel electrode was prepared via *in situ* polymerization of ANI using ammonium peroxydisulphate, in the presence of binary G/Fe_2O_3. The presence of Fe_2O_3 nanoparticles within the Gn layers can help in preventing the agglomeration of PANI nanoparticles, and thus increasing the electrochemical performance of the electrode. Moreover, the presence of Fe_2O_3 nanoparticles also inhibits the restacking of the carbon sheets and subsequently improves the faradaic movement. The PANI nanoparticles themselves act as pseudocapacitance, which contributes to the improvement in the total capacitance. Further, they showed that the synergistic effect of the three components in the PANI/RGO/Fe_2O_3@CC is perceptible compared to other electrode materials consisting of G/PANI or Fe_2O_3/RGO. The G/PANI@CC electrode only yielded a specific capacitance of 793 F/g at 0.5 A/g in 1 M H_2SO_4 electrolyte,[35] while the Fe_2O_3/RGO@CC only achieved a specific capacitance of 255 F/g at 0.5 A/g in 1 M Na_2SO_4.[98] The low specific capacitance of Fe_2O_3/RGO is also partly attributed to the electrolyte solution; for example, in a similar material of study with PANI/RGO/Fe_2O_3@CC, the SC electrode from G/Fe_2O_3/PANI (Gn was used instead of RGO) was only able to achieve a specific capacitance of 638 F/g using KOH electrolyte.[49]

Yasoda et al.[25] demonstrated that using Mn_3O_4 nanoflakes to fabricate GO/PANI could result in the high-performance SC electrode with a specific capacitance of 829 F/g at 0.3 A/g in 1 M H_2SO_4. Meanwhile, only a specific capacitance of 335 F/g can be achieved without the presence of Mn_3O_4 in the electrode matrix. The inclusion of mechanical stirring was reported to cause a decrease in specific capacitance to 643 F/g. The usage of rare transition metal oxides, such as RuO_2, to fabricate SC electrodes is reported to produce electrodes with theoretical high specific capacitance values between 1400 and 2000 F/g. However, the major drawbacks of using RuO_2 lie in its expensive cost, low abundance, and high agglomeration tendency. Although the hybridization of RuO_2 with carbon-based materials can help address the agglomeration issue, the high cost of this TMO remains the main barrier for its commercial application.[23] The addition of PANI into RuO_2/G composites can further improve the capacitance of the resultant electrodes. For example, Rakhi et al.[99] showed that the electrode material prepared from chemically anchored RuO_2 particles onto Gn nanosheets could achieve a specific capacitance of 365 F/g under a scan rate of 20 mV/s. Ates and Yildrim[39] also reported an almost 2-fold increase in the specific capacitance of the RGO/RuO_2 electrode upon the incorporation of PANI. In this case, the hybrid electrode prepared from RuO_2/RGO/PANI achieved a specific capacitance

of 723.09 F/g at 2 mV/s and maintained 85.14% of its initial capacitance after 1,000 cycles. On the other hand, the SC electrodes fabricated from RGO/RuO_2, RGO/PANI, and RuO_2/PANI all displayed lower specific capacitances of 347.28 F/g, 159.62 F/g, and 40.2 F/g, respectively, while pure RGO-based electrode only reached 37.5 F/g.

The usage of binary metal oxide of Co/Fe has been shown to produce hybrid electrode materials with a superior specific capacitance value. Xiong et al.[30] demonstrated that a ternary combination of $CoFe_2O_4$/G/PANI results in an electrode material possessing a specific capacitance of ~1,133.3 F/g at a scan rate of 1 mV/s and 767.7 F/g at a current density of 0.1 A/g. By comparison, the binary electrode comprising G/PANI only achieved ~716.4 F/g (at 1 mV/s) and 329.3 F/g (at 0.1 A/g). Moreover, the ternary composite electrode exhibits a superior long-term cycling performance, maintaining 96% capacitance after 5,000 cycles. Similar results were obtained by Mousa et al.,[100] which reported a slightly higher specific capacitance value (i.e., 1,123 F/g at 1 mV/s) of $CoFe_2O_4$/G/PANI electrode but slightly inferior cycling stability performance (98.2% retention over 2,000 cycles). The hybridization of G/PANI electrodes with other TMOs has been extensively investigated; however, the resultant electrode materials possess much lower specific capacitance, namely 325 F/g (Fe_3O_4/G/PANI) and 645 F/g ($NiFe_2O_4$/G/PANI). Very recently, Shaheen et al.[52] reported that the utilization of ternary TMOs of $NiPbTiO_3$ could dramatically increase the specific capacitance of the RGO/PANI hybrid. The $NiPbTiO_3$/RGO/PANI hybrid can achieve a specific capacitance of 1,180 F/g (at 0.5 A/g), while pure PANI and $NiPbTiO_3$ only afforded 800 F/g (at 13 A/g) and 384 F/g (at 5 A/g), respectively.

The major drawback of using TMOs in the fabrication of the SC electrodes is the poor cycling stability. The free-standing TMOs and G/PANI/TMO electrodes commonly have cycling stability between 200 and 5,000 cycles, due to the volume change of TMOs in the electrolyte solution during the electrochemical process.[96] The addition of carbon-based substrates, such as CC, represents an effective means to address this issue. For instance, growing the PANI/RGO/Fe_2O_3@CC substrate can result in 10,000 cycling stability. By contrast, the free-standing G/Fe_2O_3/PANI and Mn_3O_4/GO/PANI without CC only exhibited 5,000 and 1,800 cycling stability, respectively. Although the combination of TMOs/G/PANI can be promising for preparing energy storage devices with high specific capacitance, the high cost and low abundance of several TMOs, and the possibility of metal toxicity to the environment, need to be further considered for practical applications.

The utilization of MOFs for preparing SC electrodes has started to emerge. Since introduced in 1995 by Yaghi et al.,[101] MOFs have gained significant interest from scientific communities in various fields. MOF possesses a large specific surface area and high porosity as an electrode material, accommodating the electrolyte ions and acting as the redox-active sites. MOF materials prepared from the combination of H_3BTC, H_2BDC, and PTA with various transition metals (e.g., Ni, Co, Mn, and Fe) have been widely used for preparing the SC electrode. The MOFs are usually combined with carbon-based material or CPs, and the reported electrodes can reach a specific capacitance up to 1,800 F/g and cycling stability up to 10,000 cycles.[102] Several high specific capacitance MOF-contained electrodes have been reported. For example, Saraf et al.[103] reported that a combination of Cu-MOF/RGO/GCE can result in a hybrid electrode with a specific capacitance of 685 F/g (in 1 M Na_2SO_4 at a current density of 1.6 A/g). Meanwhile, the Cu-MOF/GCE and RGO/GCE electrodes are only able to achieve specific capacitance of 85 F/g, 410 F/g and 685 F/g, respectively. The hybridization of CNT with Ni-MOF is reported to result in an electrode with a specific capacitance of 1,765 F/g (in 6 M KOH, at a current density of 0.5 A/g), which is higher than the Ni-MOF (1,080 F/g).[104] Composite electrode from the combination of MOF with carbon-based materials is shown to have higher specific capacitance than the electrode prepared from MOF alone. The enhancement of the specific capacitance can be related to the better diffusion of electrolyte ions and electron transport in the composite electrode. To date, there is still no study that shows the electrochemical performance of the combination of MOF/G/PANI, and therefore, no information can be gathered.

3.2 *Surface functionalization approaches*

The combination of functionalized-Gn and PANI has been reported to produce SC electrodes with great specific capacitance values. In this regard, N- and S-contained functional groups, such as amine and sulfonate, are frequently used to modulate the surface chemical characteristics of Gn nanomaterial.[105] The incorporation of such functional groups has been demonstrated in several studies to play a role in controlling the morphology of PANI nanostructures anchored on the Gn plane. In this section, the preparation and performance of several functionalized-Gn/PANI hybrid electrodes are summarized and discussed, along with the critical factors that influence the electrocapacitive properties of the resultant hybrid electrodes.

The usage of S,N:GQDs along with PANI (PANI/S,N:GQDs) resulted in the SC electrode with an ultrahigh specific capacitance of 2,524 F/g at a current density of 2 A/g, showing a 2.5-fold enhancement in the capacitance compared to that of GQDs/PANI electrode.[46] In this study, the S,N:GQD was prepared via a hydrothermal method using citric acid as a carbon precursor and thiourea (CH_4N_2S) as the S,N-source. The PANI/S,N:GQDs composite materials are then obtained by mixing S,N:GQDs with ANI and followed by ANI polymerization in the presence of APS. A conductive mixture composed of 80 wt% PANI/S,N:GQDs, 10 wt% carbon black, 10 wt% PVDF, 0.3 mL $_N$-methyl-2-pyrrolidone, and 0.3 mL ethanol was then painted on 1 × 4.5 cm^2 Ni-foam to prepare the SC electrode. Ramadan et al.[46] also reported that the aggregation of GQDs in the composites tends to occur at high GQDs content, causing the formation of many void spaces and decreasing the electrochemical performance of the electrode. The combination of 10 mg S,N:GQDs/PANI resulted in an SC electrode with the highest specific capacitance. Interestingly, the addition of 10 mg PANI/S,N:GQDs resulted in an electrode with the lower surface area than pure PANI, which is 21.9 and 30.8 m^2/g for PANI/S,N:GQDs and PANI, respectively. Although pure PANI has a higher BET surface area, its specific capacitance only reached 1080 F/g, which is 2.3 times lower than PANI/S,N:GQDs. The reduction in the BET surface area of PANI/S,N:GQDs can be attributed to the intercalation of the S,N:GQDs into the PANI matrix, which can facilitate the mobility of electrons and ions and thus enhance the electrochemical performance of the electrode.

In an earlier study, Liu et al.[106] demonstrated a comparison study toward the specific capacitance values of SC hybrid electrodes prepared from the combination of PANI with GO, RGO, N-Gn, and S-Gn. The composite electrode materials are constructed of multilayer stacking of PANI nanorods grown on micron-sized graphene sheets. More homogeneous growth of PANI nanorods were observed when the aniline monomers were paired with S-Gn. The sulfonate groups have higher electronegative intensities than the hydroxylamine groups in GO and Gn, thus stimulating the nucleation and uniform growth of PANI nanorods. The results showed that PANI/S-Gn composites exhibit the largest BET surface of 49.0 m^2/g, while other composites possess a lower BET surface area ranging from 20.2 to 36.6 m^2/g. According to XPS analysis, pure PANI and PANI/S-Gn show a high total content of -N= and $-NH^+$ (i.e., ~50%), giving rise to the electrical conductivity of the electrode. The highest specific capacitance of 863.2 F/g at 0.2 A/g and rate capability of 67.4% (581.6 F/g at 5 A/g) can be achieved by using PANI/S-Gn composites.

In another work, Ke et al.[107] reported a PANI/ATRGO hybrid electrode with a flower-like morphology that displays an impressive specific capacitance of 1,510 F/g at a current density of 1 A/g and 89% cycling stability after 1,500 cycles. ATRGO was prepared through modification of GO with TCTA and *p*-phenylenediamine. Then, 2-10 wt% of ATRGO was mixed with ANI in 1 M H_2SO_4 to produce PANI/ATRGO composite. The highest specific capacitance of this composite material was obtained at 5 wt% ATRGO loading, resulting in the formation of homogenous flower-like PANI nanosheets anchored on graphene. In this regard, the homogenous growth of PANI nanosheets was not able to achieve at lower ATRGO. Higher loading amounts of ATRGO than 5 wt% gave disordered stacking of PANI nanosheets on the Gn surface. Such the morphologies and non-homogenous distribution of PANI nanosheets on Gn lead to the lower specific capacitance values of 697 and 1,216 F/g for PANI/ATRGO 2 wt% and PANI/ATRGO 10 wt%, respectively.

The preparation of a GOF/PANI hybrid electrode has been reported by Y. Li et al.[108] The GOF was prepared by mixing carboxylated-GO with Selectfluor (1-chloromethyl-4-fluoro-1,4-diazoniabicyclo[2.2.2]octane, a fluorine donor chemical) and $AgNO_3$ in water. Then, 3% of freeze-dried GOF was mixed with ANI at a weight ratio of 3 : 100, followed by an oxidation polymerization to produce GOF/PANI composites. The as-synthesized GOF/PANI can achieve a specific capacitance of 502 F/g at 1.0 A/g and maintain 95% cycling stability after 600 cycles. The GOF/PANI nanocomposite is constructed of densely packed granular PANI on the GOF plane. Furthermore, agglomeration of the PANI particles was also found in some regions of the nanocomposites; the PANI particles that are not nanosized are likely to cause the reduction of the specific capacitance and poor cycling cycles. In this regard, an SC electrode material with smoother morphology and nanosized PANI particles has been demonstrated to deliver enhanced cycling stability and higher specific capacitance, as proven in the recent study by Li et al.[109]

The combination of PAG/PANI resulted in an SC electrode with a specific capacitance of 1,092.3 F/g under a scan rate of 5 mV/s.[109] This amine group functionalized electrode was constructed by growing the PANI nanoarrays on the PAG. In this regard, PAG was prepared from the oxidation of graphite through the Hummers method, followed by chemical reduction using hydrazine. The resulting Gn nanosheets were then mixed with 1,4-benzenediamine in $NaNO_2$/H_2SO_4 solution to obtain PAG. The PAG/PANI active material was then prepared by mixing 20 wt% PAG with 0.91 mL ANI and ~1.4 g NSA in 100 mL of 1 M HCl solution. Polymerization of ANI into PANI was performed by using

APS for 8 h. Another hybrid composite, namely PAG/PANI-w, uses water instead of 1 M HCl solution. However, the resultant PAG/PANI-w composite only achieved a specific capacitance of 585.0 F/g, much lower than PAG/PANI (1,092.3 F/g) and pure PANI (898.5 F/g). The higher specific capacitance values of pure PANI and PAG/PANI electrodes than PAG/PANI-w can be attributed to the doping effect of PANI by HCl.

A solid-state SC, namely G-PC, with a tremendous specific capacitance of 1,701.1 F/g at a scan rate of 5 mV/s, has been reported in another study by Li et al.[110] The G-PC has an energy density of 15.3 Wh/kg (at a power density of 50 W/kg) and outstanding capacitance retention of 94.9% after 5,000 cycles. Such a remarkable specific capacitance is achieved by combining NH_2-GNS, ANI, PPDA, and TPA. The NH_2-GNS were prepared by using the same previously reported method.[109] The resultant NH_2-GNS was then mixed with ANI, PPDA, and TPA to synthesize the G-PC nanocomposite. It was shown that incorporating the amine functional group causes an increase in the C and N contents while lowering the O content of Gn; the lower O content can help to reduce the moisture of Gn. The authors also showed that the loading content of NH_2-GNS significantly affects the surface morphology of the resulting nanocomposites. The PANI particles form a nanofibrous structure, resulting in a smoother surface than previously reported PAG/PANI.[109-110] In this regard, a quite uniform distribution of PANI-copolymer on the GNS was obtained at GNS-NH_2 weight loadings ranging from 10 to 30 wt%. Higher NH_2-GNS loadings of ca. 50 wt% resulted in the formation of the disordered nanofibrous structure of PANI with some large cavities, making it not suitable for efficient diffusion of the electrolyte ions and charge transport. The highest specific capacitance of 1,701.1 F/g was achieved with an NH_2-GNS mass loading of 20%, whereas higher and lower loading amounts result in lower capacitance values of 1,141.9-1,242.7 F/g. The electrode materials prepared without the addition of NH_2-GNS and unfunctionalized GNS exhibited an evenly low specific capacitance of 859.2 F/g and 882.6 F/g, respectively.

3.3 *Gn-based hybrid composites with other CPs*

3.3.1 *G/PPy nanocomposites*

PPy is one of the most widely used p-type CPs for preparing composite electrodes due to its high conductivity (10-1,000 S/cm) and ease of synthesis by chemical and electrochemical methods. Similar to other PANI cases, the grafting of carbon-derived nanomaterials to PPy can improve the cycling stability of the resultant hybrid electrodes during charge and discharge cycles. For instance, Wang et al.[111] reported a novel technique to produce a composite RGO/PPy porous electrode, based on the *in situ* galvanostatic polymerizations. The resultant composite exhibits a BET surface area of 108 m^2/g and outstanding electrochemical performance, including high specific capacitance (224 F/g at 240 A/g), energy and power densities of 2.5 Wh/kg and 38.6 kW/kg, respectively, and good cycling stability (17% capacitance loss after 5000 charge-discharge cycles). In another study, Zhang and Zhao[112] demonstrated the direct coating of PPy on RGO sheets through *in situ* polymerization process to produce PPy/RGO composite. The authors found that ethanol as a solvent can improve the dispersion of RGO sheets and subsequently promote the diffusion and growth of PPy over the RGO surface. The specific capacitance of the PPy/RGO composite electrode was 248 F/g at 0.3 A/g with capacitance retention of 80% over 1,000 cycles of charge/discharge.

The hydrothermal method has also been utilized by Gu et al.[113] to prepare a 3D RGO/PPy composite hydrogel. In this study, $KMnO_4$ was used as the oxidant in the polymerization of pyrrole monomers to form PPy on the surface of GO sheets at 95 °C for 24 h. Under this polymerization condition, GO sheets are reduced and subsequently self-assembled to create a 3D porous structure. The SSA of the PPy/RGO composite hydrogel was 331 m^2/g, yielding a specific capacitance of 356 F/g. The capacitance properties of the as-prepared composites were influenced by the uniformity and thickness of the PPy coating on Gn. Sun et al.[114] employed a spontaneous assembly or *in situ* redox process without an external oxidizing or reducing agent to produce 3D RGO/PPy hybrid aerogels for SC electrodes. The composite with excellent electrochemical performance (specific capacitance of 230.8 F/g at 1 A/g, and retention of 58.26% after 50 cycles) and mechanical properties was obtained using their method. The strong π-π interaction between PPy and RGO is responsible for the excellence of the mechanical property of the composite. A recent study by Zhang et al.[59] shows a clear correlation between the specific surface area and the specific capacitance of the resulting electrode made of freestanding PPy@RGO hydrogel. The specific surface area of the PPy@RGO hydrogel (hereinafter referred to as PPy@RGOH) can be modulated by varying the electropolymerization time of PPy from 0 to 30 s. The PPy@RGOH obtained at an electrochemical polymerization time of 20 s (i.e., PPy@RGOH-20 s) possesses the highest specific surface area of 231.2

m^2/g, while the PPy@RGOH-10 s and PPy@RGOH-30 s only exhibited 164.7 and 152.0 m^2/g, respectively. The specific surface area values of PPy@RGOH composites are influenced by the formation of aggregates of the active electrode materials (e.g., RGO and PPy). A severe aggregation of these active materials can lead to the destruction of the electrode network structure, thus reducing the rate of charge transfer and decreasing the specific capacitance of the electrode. Furthermore, the aggregation of CPs is generally observed to be more at excessive loading amounts.[112,115-116]

3.3.2 *Gn nanocomposites with PTh and their derivatives*

The combination of PTh and GNS as SC electrode materials has been demonstrated in several studies, although the number of publications is relatively more minor compared to those using PANI and PPy. Among various PTh derivatives, highly conductive PEDOT is of particular interest for preparing high-performance SC electrode materials. For example, Lee et al. reported the fabrication of a thin multilayer G/PEDOT film using an *in situ* electrochemical deposition method.[117] SEM analysis proves the successful deposition of the G/PEDOT multilayers. The specific capacitance value of the composite thin film with six Gn layers was found to be 154 F/g, and this value decreased slightly to 132.44 F/g (86% capacitance retention) after 1,000 charge and discharge cycles. Zhang and Zhao also employed PEDOT to fabricate RGO/PEDOT composite for high-performance SC electrodes. In their study, PEDOT was directly coated on RGO sheets via an *in situ* polymerization process.[112]

Ates et al. demonstrated the fabrication of a ternary composite material from the combination of RGO, Ag, and PTh (RGO/Ag/PTh).[64] The electrode with a specific capacitance of 953.13 F/g (at a scan rate of 4 mV/s) was achieved at a GO/Th ratio of 0.2. The prepared ternary nanocomposite also displayed excellent cycling stability (91.88%) after 1,000 charging/discharging cycles. Azimi et al.[118] investigated the electrochemical properties of several PTh nanocomposites with GO and RGO. They found that incorporating GO and RGO to PTh nanoparticles could enhance the electrochemical properties of the resultant electrodes. Specifically, the specific capacitance of GO/PTh, RGO/PTh, and PTh at a scan rate of 5 mV/s was 16.39 F/g, 28.68 F/g, and 3.5 F/g, respectively.

4. Summary and future perspective

In summary, the development and breakthrough of the researches in the improvement of the electrochemical properties and cycling stability of the G/PANI hybrid electrodes have been reviewed.

Incorporating Gn can facilitate the homogeneous distribution of PANI nanoparticles, thereby resulting in an SC electrode with better electrochemical properties. The synergistic effect of G/PANI comes from the π-π stacking interaction between the aromatic rings or the two compounds (Figure 3a), which boosts the electrode conductivity by facilitating the electron donor-acceptor transfer (Figure 3b). Through detailed analysis on the properties of G/PANI hybrid electrode, it can be postulated that three factors should be considered to produce electrodes with enhanced capacitance and cycling stability, including 1) composition and the ratio of Gn and PANI; 2) morphology, structure, and size of the materials; 3) hybridization with other materials.

The proper amount of Gn and PANI is a crucial aspect to prevent the aggregation of the electrodes particles, and to control the morphologies and size of the particles. This effect is reported in work by Xia et al.[49] The SC electrodes prepared at a low amount of PANI, i.e., $(G/Fe_2O_3/PANI)_{0.5}$ prepared from G/Fe_2O_3 to ANI at the ratio of 2:1, can achieve a specific capacitance of 638 F/g (Figure 4a). Meanwhile, the specific capacitance is decreased for 1.7-3.2 times at high G/Fe_2O_3 to ANI at the ratio of 1:1, 1:5, and 1:10, repectively; where the resultant electrode coded as $(G/Fe_2O_3/PANI)_1$, $(G/Fe_2O_3/PANI)_5$, $(G/Fe_2O_3/PANI)_{10}$, respectively.[49] The significant decrease in specific capacitance was due to the occurrence of aggregation, which inhibits the smooth ion transfer within the electrode matrix. Higher specific capacitance also can be achieved by combining several conducting materials. The usage of single electrode particles, such as Gn, PANI, and Fe_2O_3, only resulted in a low specific capacitance of 33-198 F/g (Figure 4a). Meanwhile, combining the three materials can significantly enhance the specific capacitance to 638 F/g.[49]

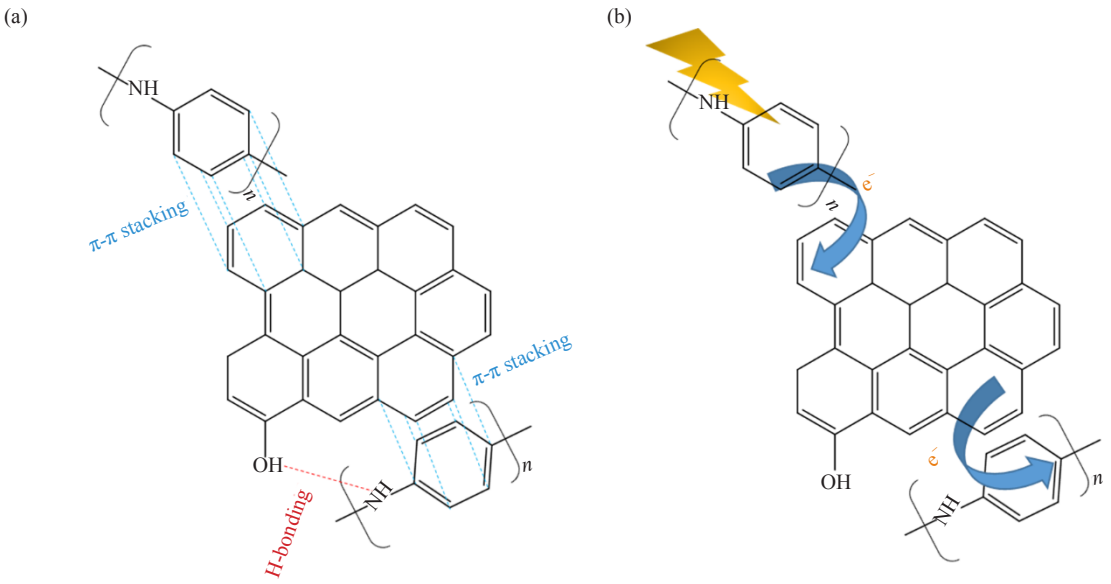

Figure 3. (a) Schematic illustration showing the bonding interaction between PANI and RGO. (b) Charge transfer process between PANI and RGO

The establishment of material with nanosize, homogenous structure, and controlled morphologies is a crucial point in producing SC with excellent properties. The introduction of conductive materials (e.g., TMOs and MOFs) and/or functionalization of the materials are approaches that can be employed as a strategy to enhance the electrochemical properties of SC. The usage of TMOs may result in higher specific capacitance value and better electron transport for the electrode; however, their high cost, low availability, and high toxicity risk are major challenges for their application. The type of TMOs also plays a vital role in affecting the electrochemical properties of the resulting electrode. As shown in Figure 4b, a different value of specific capacitance was obtained by using a different type of single TMOs. The usage of binary TMOs (instead of single TMOs) can enhance the specific capacitance of the electrode. Nevertheless, many TMO combinations are available and waiting to be studied. Therefore, a complete understanding of the properties and conductivity of each TMO will help in determining the best binary combination. Other strategies to enhance the specific capacitance of the electrode include the incorporation of MOFs and surface functionalization of Gn. The incorporation of MOFs can assist in increasing the SSA and porosity of the electrodes, thereby facilitating the diffusion of electrolyte ions; however, the high cost and complexity of the MOFs production process is still a challenge. Surface functionalization of Gn was also postulated as one of the strategies for achieving high-performance electrodes. However, the poor cycling cycle and the tendency of particles agglomeration often hindered their industrial-scale application. While each strategy has its advantages and disadvantages, one should review the intended use of SC to determine the best electrode composition.

Numerous promising methods and approaches to improve the performance of G/PANI hybrid electrodes have been demonstrated; however, there are still many challenges and research gaps awaiting to be answered. Although thousands of works related to G/PANI hybrid electrodes have been published, only hundreds of them demonstrated SC with cycling stability >10,000 cycles. While studies of SC preparations with various combinations of materials (including materials not discussed in this review) are progressing rapidly, the knowledge about the fundamental charge-discharging mechanism for these new SC combinations is still limited. Therefore, it is still a challenge to optimally design SCs materials with excellent electrochemical properties and should be the focus of future research.

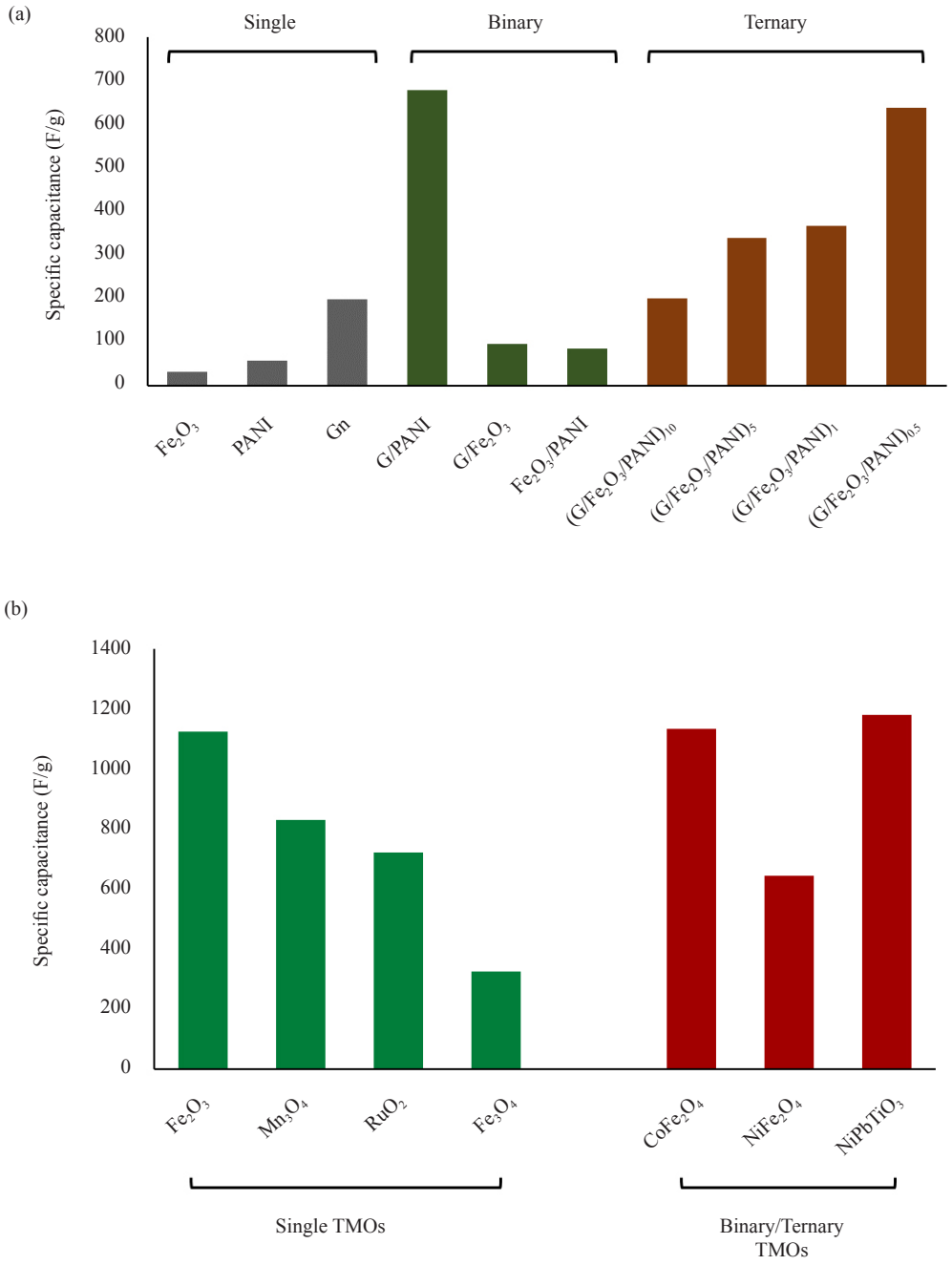

Figure 4. (a) Comparison of the specific capacitance of some G/PANI electrodes with various TMOs added, adapted from Ref. 49 (b) Comparison of the specific capacitance of single, binary, and ternary hybrid electrodes comprised of Gn, PANI, and Fe_2O_3, adapted from Refs. 25, 30, 50, 52, 98-100

Acknowledgment

This project was supported by Widya Mandala Surabaya Catholic University through an internal research grant.

Conflict of interest statement

The authors declare that there is no conflict of interest.

References

[1] Simon, P.; Gogotsi, Y.; Dunn, B. *Science* **2014,** *343*, 1210-1211.
[2] Winter, M.; Brodd, R. J. *Chem. Rev.* **2004,** *104*, 4245-4269.
[3] Zhang, L. L.; Zhao, X. S. *Chem. Soc. Rev.* **2009,** *38*, 2520-2531.
[4] Shao, Y.; Li, J.; Li, Y.; Wang, H.; Zhang, Q.; Kaner, R. B. *Mater. Horiz.* **2017,** *4*, 1145-1150.
[5] Dubal, D. P.; Chodankar, N. R.; Kim, D.-H.; Gomez-Romero, P. *Chem. Soc. Rev*. **2018,** *47*, 2065-2129.
[6] Liu, L.; Zhao, Z.; Hu, Z.; Lu, X.; Zhang, S.; Huang, L.; Zheng, Y.; Li, H. *Front. Chem.* **2020,** *8*, 371-371.
[7] Tian, Z.; Tong, X.; Sheng, G.; Shao, Y.; Yu, L.; Tung, V.; Sun, J.; Kaner, R. B.; Liu, Z. *Nat. Commun*. **2019,** *10*, 4913-4913.
[8] Forouzandeh, P.; Kumaravel, V.; Pillai, S. C. *Catalysts* **2020,** *10*, 969.
[9] Palchoudhury, S.; Ramasamy, K.; Gupta, R. K.; Gupta, A. *Front. Mater.* **2019,** *5*, 83.
[10] Moyseowicz, A.; Gryglewicz, G. *Compos. B. Eng.* **2019,** *159*, 4-12.
[11] Wang, M.; Xu, Y.-X. *Chin. Chem. Lett.* **2016,** *27*, 1437-1444.
[12] Ke, Q.; Wang, J. *J. Materiomics.* **2016,** *2*, 37-54.
[13] Lekakou, C.; Moudam, O.; Markoulidis, F.; Andrews, T.; Watts, J. F.; Reed, G. T. *Nanocomposites* **2011,** *2011*, 409382.
[14] Zhang, L.; Yang, X.; Zhang, F.; Long, G.; Zhang, T.; Leng, K.; Zhang, Y.; Huang, Y.; Ma, Y.; Zhang, M.; Chen, Y. *J. Am. Chem. Soc.* **2013,** *135*, 5921-5929.
[15] Viswanathan, B. Supercapacitors. In *Energy Sources: Fundamentals of Chemical Conversion Processes and Applications*, John Fedor: Elsevier B.V., 2017; pp 315-328.
[16] Meng, Q.; Cai, K.; Chen, Y.; Chen, L. *Nano Energ.* **2017,** *36*, 268-285.
[17] Muzaffar, A.; Ahamed, M. B.; Deshmukh, K.; Thirumalai, J. *Renew. Sustain. Energy Rev.* **2019,** *101*, 123-145.
[18] Sinha, P.; Kar, K. K. Introduction to Supercapacitors. In *Handbook of Nanocomposite Supercapacitor Materials II*, Kar, K. K., Ed. Springer Nature Switzerland AG: Switzerland, 2020; Vol. 302.
[19] Liu, Z.; Zhang, S.; Wang, L.; Wei, T.; Qiu, Z.; Fan, Z. *Nano. Select.* **2020,** *1*, 244-262.
[20] Balli, B.; Şavk, A.; Şen, F. Graphene and polymer composites for supercapacitor applications. In *Nanocarbon and its Composites: Preparation, Properties and Applications*, Khan, A.; Jawaid, M.; Inamuddin; Asiri, A. M., Eds. Woodhead Publishing Series in Composites Science and Engineering: Elsevier, 2019; pp 123-151.
[21] Sur, U. K. *Int. J. Chem.* **2012,** *2012*, 237689.
[22] Drieschner, S.; Weber, M.; Wohlketzetter, J.; Vieten, J.; Makrygiannis, E.; Blaschke, B. M.; Morandi, V.; Colombo, L.; Bonaccorso, F.; Garrido, J. A. *2D Mater.* **2016,** *3*, 045013.
[23] Majumdar, D.; Maiyalagan, T.; Jiang, Z. *Chem. Electro. Chem.* **2019,** *6*, 4343-4372.
[24] Liu, C.; Yu, Z.; Neff, D.; Zhamu, A.; Jang, B. Z. *Nano. Lett.* **2010,** *10*, 4863-4868.
[25] Yasoda, K. Y.; Kumar, M. S.; Batabyal, S. K. *Ionics* **2020,** *26*, 2493-2500.
[26] Mondal, S.; Rana, U.; Malik, S. *Chem. Commun.* **2015,** *51*, 12365.
[27] Zhang, M.; Wang, X.; Yang, T.; Zhang, P.; Wei, X.; Zhang, L.; Li, H. *Synth. Met.* **2020,** *268*, 116484.
[28] Li, K.; Liu, X.; Chen, S.; Pan, W.; Zhang, J. *J. Energy Chem.* **2019,** *32*, 166-173.
[29] Gomez, H.; Alvi, F.; Villalba, P.; Ram, M. K.; Kumar, A. In *Supercapacitor Based on Graphene-Polyaniline Nanocomposite Electrode*, Mater. Res. Soc. Symp. Proc., Materials Research Society, 2011.
[30] Xiong, P.; Huang, H.; Wang, X. *J. Pow. Sour.* **2014,** *245*, 937-946.
[31] Cong, H.-P.; Ren, X.-C.; Wang, P.; Yu, S.-H. *Energy Environ. Sci.* **2013,** *6*, 1185.
[32] Zhang, T.; Yue, H.; Gao, X.; Yao, F.; Chen, H.; Lu, X.; Wang, Y.; Guo, X. *Dalton Trans.* **2020,** *49*, 3304-3311.
[33] Lin, Y.; Zhang, H.; Deng, W.; Zhang, D.; Li, N.; Wu, Q.; He, C. *J. Power Sources* **2018,** *384*, 278-286.
[34] Jin, C.; Wang, H.-T.; Liu, Y.-N.; Kang, X.-H.; Liu, P.; Zhang, J.-N.; Jin, L.-N.; Bian, S.-W.; Zhu, Q. *Electrochim. Acta* **2018,** *270*, 205-214.
[35] Wen, L.; Li, K.; Liu, J.; Huang, Y.; Bu, F.; Zhao, B. *RSC Adv.* **2017,** *7*, 7688-7693.
[36] Chen, N.; Ni, L.; Zhou, J.; Zhu, G.; Kang, Q.; Zhang, Y.; Chen, S.; Zhou, W.; Lu, C.; Chen, J.; Feng, X.; Wang, X.; Guo, X.; Peng, L.; Ding, W.; Hou, W. *ACS Appl. Energy Mater.* **2018,** *10*, 5189-5197.

[37] Mitchell, E.; Candler, J.; Souza, F. D.; Gupta, R. K.; Gupta, B. K.; Dong, L. F. *Synth. Met.* **2015,** *199*, 214-218.
[38] Xu, H.; Zhu, Y.; Zhang, M.; Li, Q.; Zuo, S.; Chen, Y. *Ionics* **2020,** *26*, 5199-5210.
[39] Ates, M.; Yildrim, M. *Polym. Bull.* **2020,** *77*, 2285-2307.
[40] Yang, Y.; Xi, Y.; Li, J.; Wei, G.; Klyui, N. I.; Han, W. *Nanoscale Res. Lett.* **2017,** *12*, 394.
[41] Hong, X.; Zhang, B.; Murphy, E.; Zou, J.; Kim, F. *J. Pow. Sour.* **2017,** *343*, 60-66.
[42] Hu, R.; Zhao, J.; Zhu, G.; Zheng, J. *Electrochim. Acta* **2018,** *261*, 151-159.
[43] Luo, Y.; Zhang, Q. E.; Hong, W.; Xiao, Z.; Bai, H. *Phys. Chem. Chem. Phys.* **2018,** *20*, 131-136.
[44] Yu, P.; Zhao, X.; Huang, Z.; Li, Y.; Zhang, Q. *J. Mater. Chem. A* **2014,** *2*, 14413-14420.
[45] Wang, H.; Zhang, Y.; Li, Z.; Wu, Y.; Wu, L.; Jin, Z. *Ionics* **2020,** *26*, 4031-4038.
[46] Ramadan, A.; Anas, M.; Ebrahim, S.; Soliman, M. *J. Mater. Sci. Mater. Electron.* **2020,** *31*, 7247-7259.
[47] Yu, P.; Li, Y.; Zhao, X.; Wu, L.; Zhang, Q. *Langmuir* **2014,** *30*, 5306-5313.
[48] Wang, L.; Ye, Y.; Lu, X.; Wen, Z.; Li, Z.; Hou, H.; Song, Y. *Sci. Rep.* **2013,** *3*, 3568.
[49] Xia, X.; Hao, Q.; Lei, W.; Wang, W.; Sun, D.; Wang, X. *J. Mater. Chem.* **2012,** *22*, 16844-16850.
[50] Gupta, A.; Sardana, S.; Dalal, J.; Lather, S.; Maan, A. S.; Tripathi, R.; Punia, R.; Singh, K.; Ohlan, A. *ACS Appl. Energy Mater.* **2020,** *3*, 6343-6446.
[51] Etana, B. B.; Ramakrishnan, S.; Dhakshnamoorthy, M.; Saravanan, S.; Ramamurthy, P. C.; Demissie, T. A. *Mater. Res. Express* **2020,** *6*, 125708.
[52] Shaheen, F.; Ahmad, R.; Sharif, S.; Habib, M.; Sharif, R.; Fatima, M.; Wang, C. *Mater. Lett.* **2021,** *284*, 129031.
[53] Shafi, P. M.; Ganesh, V.; Bose, A. C. *ACS Appl. Energy Mater.* **2018,** *1*, 2802-2812.
[54] Prasankumar, T.; Vigneshwaran, J.; Abraham, S.; Jose, S. P. *Mater. Lett.* **2019,** *238*, 121-125.
[55] Abdah, M. A. A. M.; Razali, N. S. M.; Lim, P. T.; Kulandaivalu, S.; Sulaiman, Y. *Mater. Chem. Phys.* **2018,** *219*, 120-128.
[56] Han, Y.; Zhang, Z.; Yang, M.; Li, T.; Wang, Y.; Cao, A.; Chen, Z. *Electrochim. Acta* **2018,** *289*, 238-247.
[57] Kwon, H.; Han, D. J.; Lee, B. Y. *RSC Adv.* **2020,** *10*, 41495-41502.
[58] Bhargava, P.; Liu, W.; Pope, M.; Tsui, T.; Yu, A. *Electrochim. Acta* **2020,** *358*, 136846.
[59] Zhang, X.; Zhang, J.; Chen, Y.; Cheng, K.; Yan, J.; Zhu, K.; Ye, K.; Wang, G.; Zhou, L.; Cao, D. *J. Colloid Interface Sci.* **2019,** *536*, 291-299.
[60] Zhou, H.; Zhai, H.-J.; Zhi, X. *Electrochim. Acta* **2018,** *290*, 1-11.
[61] Miankushki, H. N.; Sedghi, A.; Baghshahi, S. *J. Solid State Electrochem.* **2018,** *22*, 3317-3329.
[62] Yao, T.; Li, Y.; Liu, D.; Gu, Y.; Qin, S.; Guo, X.; Guo, H.; Ding, Y.; Liu, Q.; Chen, Q.; Li, J.; He, D. *J. Power Sources* **2018,** *379*, 167-173.
[63] Alabadi, A.; Razzaque, S.; Dong, Z.; Wang, W.; Tan, B. *J. Power Sources* **2016,** *306*, 241-247.
[64] Ates, M.; Caliskan, S.; Ozten, E. *Fuller. Nanotub. Car. N* **2018,** *26*, 360-369.
[65] Liu, F.; Xie, L.; Wang, L.; Chen, W.; Wei, W.; Chen, X.; Luo, S.; Dong, L.; Dai, Q.; Huang, Y.; Wang, L. *Nano-Micro. Lett.* **2020,** *12*, 17.
[66] Arthisree, D.; Madhuri, W. *Int. J. Hydrog. Energy* **2020,** *45*, 9317-9327.
[67] Zhang, S.; Li, Y.; Song, H.; Chen, X.; Zhou, J.; Hong, S.; Huang, M. *Scientific Reports* **2016,** *6*, 19292.
[68] Chen, W.; Lv, G.; Hu, W.; Li, D.; Chen, S.; Dai, Z. *Nanotechnol. Rev.* **2018,** *7*, 157-185.
[69] Ray, S. C. Application and Uses of Graphene. In *Applications of Graphene and Graphene-Oxide Based Nanomaterials*, 2015; pp 1-38.
[70] Zhang, S.; Sui, L.; Dong, H.; He, W.; Dong, L.; Yu, L. *ACS Appl. Mater. Interfaces.* **2018,** *10*, 12983-12991.
[71] Qing, Y.; Jiang, Y.; Lin, H.; Wang, L.; Liu, A.; Cao, Y.; Sheng, R.; Guo, Y.; Fan, C.; Zhang, S.; Jia, D.; Fan, Z. *J. Mater. Chem.* **2019,** *7*, 6021.
[72] Ali, B. A.; Biby, A. H.; Allam, N. K. *Chem. Electro. Chem.* **2020,** *7*, 1672-1678.
[73] Ramadan, A.; Anas, M.; Ebrahim, S.; Soliman, M.; Abou-Aly, A. I. *Int. J. Hydrog. Energy* **2020,** *45*, 16254-16265.
[74] Wang, H.; Yan, X.; Piao, G. *Electrochim. Acta* **2017,** *231*, 264-271.
[75] Oskueyan, G.; Lakouraj, M. M.; Mahyari, M. *Carbon Lett.* **2021,** 31, 269-276.
[76] Nita, C.; Zhang, B.; Dentzer, J.; Ghimbeu, C. M. *J. Energy Chem.* **2021,** *58*, 207-218.
[77] Han, Y.; Ge, Y.; Chao, Y.; Wang, C.; Wallace, G. G. *J. Energy Chem.* **2018,** *27*, 57-72.
[78] Ko, S. H. *Nature Electronics* **2021,** *4*, 95-96.
[79] Xiao, F.; Yang, S.; Zhang, Z.; Liu, H.; Xiao, J.; Wan, L.; Luo, J.; Wang, S.; Liu, Y. *Sci. Rep.* **2015,** *5*, 9359.
[80] Liu, Z.; Zhao, Z.; Xu, A.; Li, W.; Qin, Y. *Journal of Alloys and Compounds* **2021,** *875*, 159931.
[81] Li, Y.; Xia, Z.; Gong, Q.; Liu, X.; Yang, Y.; Chen, C.; Qian, C. *Nanomaterials* **2020,** *10*, 1546.
[82] Shi, Y.; Peng, L.; Yu, G. *Nanoscale* **2015,** *7*, 12796-12806.

[83] Li, L.; Zhang, Y.; Lu, H.; Wang, Y.; Xu, J.; Zhu, J.; Zhang, C.; Liu, T. *Nat Commun* **2020,** *11*, 62.
[84] Tong, R.; Chen, G.; Tian, J.; He, M. *Polymers* **2019,** *11*.
[85] Zhou, X.; Chen, W.; Jiang, S.; Xiao, H.; Xu, X.; Yang, J.; Siddique, A. H.; Liu, Z. *ChemSusChem* **2021,** *14*, 938-945.
[86] Chi, K.; Zhang, Z.; Xi, J.; Huang, Y.; Xiao, F.; Wang, S.; Liu, Y. *ACS Appl. Mater. Interfaces.* **2014,** *6*, 16312-16319.
[87] Fan, W.; Zhang, C.; Tjiu, W. W.; Pramoda, K. P.; He, C.; Liu, T. *Mater. Interfaces* **2013,** *5*, 3382-3391.
[88] Trung, N. B.; Tam, T. V.; Kim, H. R.; Hur, S. H.; Kim, E. J.; Choi, W. M. *Chem. Eng. J.* **2014,** *255*, 89-96.
[89] Luo, J.; Ma, Q.; Gu, H.; Zheng, Y.; Liu, X. *Electrochim. Acta* **2015,** *173*, 184-192.
[90] Yan, Y.; Cheng, Q.; Wang, G.; Li, C. *J. Power Sources* **2011,** *196*, 7835-7840.
[91] Abu-Dief, A. M. *Journal of Nanotechnology and Nanomaterials* **2020,** *1*, 5-10.
[92] Mackenzie, J. D.; Nasu, H. The Electrical Conductivity of Transition Metal Oxide-Based Glasses. In *Physics of Disordered Materials. Institute for Amorphous Studies Series*, Adler, D.; Fritzsche, H.; Ovshinsky, S. R., Eds. Springer: Boston, MA, 1985.
[93] Biswas, D.; Das, A. S.; Mondal, R.; Banerjee, A.; Dutta, A.; Kabi, S.; Roy, D.; Singh, L. S. *Journal of Physics and Chemistry of Solids* **2020,** *144*, 109505.
[94] Ibrahim, E. M. M.; Abdel-Rahman, L. H.; Abu-Dief, A. M.; Elshafaie, A.; Hamdan, S. K.; Ahmed, A. M. *Materials Research Bulletin* **2018,** *107*, 492-497.
[95] Ibrahim, E. M. M.; Abdel-Rahman, L. H.; Abu-Dief, A. M.; Elshafaie, A.; Hamdan, S. K.; Ahmed, A. M. *Materials Research Bulletin* **2018,** *99*, 103-108.
[96] De, B.; Banerjee, S.; Verma, K. D.; Pal, T.; Manna, P. K.; Kar, K. K. Transition Metal Oxides as Electrode. In *Handbook of Nanocomposite Supercapacitor Materials II*, Kar, K. K., Ed. Springer Nature: Cham, Switzerland, 2020; Vol. Springer Series in Materials Science Volume 302, pp 89-112.
[97] Ibrahim, E. M. M.; Abu-Dief, A. M.; Elshafaie, A.; Ahmed, A. M. *Materials Chemistry and Physics* **2017,** *192*, 41-47.
[98] Zhu, Y.; Cheng, S.; Zhou, W.; Jia, J.; Yang, L.; Yao, M.; Wang, M.; Zhou, J.; Wu, P.; Liu, M. *ACS Sustainable Chem. Eng.* **2017,** *5*, 5067-5074.
[99] Rakhi, R. B.; Chen, W.; Cha, D.; Alshareef, H. N. *J. Mater. Chem.* **2011,** *21*, 16197-16204.
[100] Mousa, M. A.; Khairy, M.; Shehab, M. *J. Solid State Electrochem.* **2017,** *21*, 995-1005.
[101] Yaghi, O. M.; Li, H. *J. Am. Chem. Soc.* **1995,** *117*, 10401-10402.
[102] Huang, S.; Shi, X.-R.; Sun, C.; Duan, Z.; Ma, P.; Xu, S. *Nanomaterials* **2020,** *10*, 2268.
[103] Saraf, M.; Rajak, R.; Mobin, S. M. *Journal of Materials Chemistry A* **2016,** *4*, 16432-16445.
[104] Wen, P.; Gong, P.; Sun, J.; Wang, J.; Yang, S. *Journal of Materials Chemistry A* **2015,** *3*, 13874-13883.
[105] Hong, X.; Fu, J.; Liu, Y.; Li, S.; Wang, X.; Dong, W.; Yang, S. *Materials (Basel)* **2019,** *12*, 1451.
[106] Liu, X.; Zheng, Y.; Wang, X. *Chem. Eur. J.* **2015,** *21*, 10408-10415.
[107] Ke, F.; Liu, Y.; Xu, H.; Ma, Y.; Guang, S.; Zhang, F.; Lin, N.; Ye, M.; Lin, Y.; Liu, X. *Compos. Sci. Technol.* **2017,** *142*, 286-293.
[108] Li, Y.; Xing, R.; Zhang, B.; Bulin, C. *Polym. Polym. Compos.* **2019,** *27*, 76-81.
[109] Li, T.; Liu, P.; Gao, Y.; Diao, S.; Wang, X.; Yang, B.; Wang, X. *Mater. Lett.* **2019,** *244*, 13-17.
[110] Li, T.; Wang, X.; Liu, P.; Yang, B.; Diao, S.; Gao, Y. *J. Electroanal. Chem.* **2020,** *860*, 113908.
[111] Wang, J.; Xua, Y.; Zhu, J.; Ren, P. *J. Power Sources* **2012,** *208*, 138-143.
[112] Zhang, J.; Zhao, X. S. *J. Phys. Chem. C* **2012,** *116*, 5420-5426.
[113] Gu, X.; Yang, Y.; Hu, Y.; Hu, M.; Huang, J.; Wang, C. *J. Mater. Chem. A* **2015,** *3*, 5866-5874.
[114] Sun, R.; Chen, H.; Li, Q.; Song, Q.; Zhang, X. *Nanoscale* **2014,** *6*.
[115] Gupta, S.; Price, C. *Compos. B. Eng.* **2016,** *105*, 46-59.
[116] Wang, H.; Lin, J.; Shen, Z. X. *J. Sci. Adv. Mater. Devices* **2016,** *1*, 225-255.
[117] Lee, S.; Cho, M. S.; Lee, H.; Nam, J.-D.; Lee, Y. *J. Mater. Chem.* **2012,** *22*, 1899-1903.
[118] Azimi, M.; Abbaspour, M.; Fazli, A.; Setoodeh, H.; Pourabbas, B. *J. Electron. Mater.* **2017,** *47*, 2093-2102.